

Signatures from the spent fuel: simulations and interpretation of the data with neural network analysis

A. Borella¹, R. Rossa¹, C. Turcanu¹

¹ SCK•CEN, Nuclear Science and Technology unit,
Boeretang 200, B-2400 Mol, Belgium
Email: aborella@sckcen.be

Abstract:

In the last years, the safeguards verification of spent fuel assemblies by NDA has received increased interest also due to upcoming programmes for the geological disposal. During safeguards inspections one aims at verifying the completeness and correctness of operator declared data. One should then be able to draw conclusions on the fuel integrity and diversion of pins, as well as checking the consistency of operator declarations on initial enrichment, fuel type, burnup and cooling time. The verification of spent fuel is also important for safety aspects related to the storage of spent fuel.

The experimental observables associated to NDA of spent fuel assemblies are often a complex function of the characteristics of the fuel, its irradiation history and other variables related to the used measurement setup and devices; nowadays one often assumes that some of the variables are known to interpret the data and draw conclusions. To facilitate the interpretation of the data and draw more robust safeguards conclusions, an R&D effort is on-going at SCK•CEN and its results are given in this paper.

This work reports first about the efforts done at SCK•CEN on simulating detector response functions for different types of NDA instruments such as the Fork detector, the ForkBall detector and SINRD detectors. These responses are obtained from Monte Carlo model of the fuel and measurement setup. The spent fuel composition and radiation characteristics are taken from a spent fuel reference library developed in recent years.

A database of detector responses corresponding to 8400 cases with different fuel characteristics and irradiation parameters was then obtained. We explore the use of these simulated observables as input for data analysis algorithms aimed at uniquely characterizing the spent fuel and drawing safeguards conclusions. More specifically, we focus on the application of artificial neural networks due to their ability to generalize non-linear relationships. As a first step, cooling times smaller than 100 years were selected from the database, and several network configurations and training schemes were investigated.

Keywords: Spent fuel verification; Simulated observables; Data mining; Artificial neural network

1. Introduction

Spent fuel assemblies (SFA) are subject to verification of safeguards authorities due to their residual fissile material content. A direct measurement of the residual fissile mass is not possible with available technologies [1,2,3] and can only be estimated. The workhorses used during the verification of SFA are instruments such as the DCVD and the Fork detectors; these instruments allow to draw conclusions on the absence of gross defect in the fuel assemblies and verify the consistency of the operator declaration about fuel characteristics (e.g. fuel type, initial enrichment) and irradiation history (e.g. burnup and cooling time).

Considering the large amount of spent fuel in interim storage and the incipient opening of spent fuel repositories [4], there is an interest in developing NDA methodologies that could allow a more quantitative assessment of the spent fuel assembly before its disposal. This interest is also shared by the regulatory authorities and fuel management bodies to comply with requirements related to the safe fuel disposal; the implementation-oriented R&D activities on deep geological disposal of spent fuel and long-lived radioactive waste has been emphasised in [5,6].

The traditional nuclear signatures of spent fuel in a Non-Destructive Assay, i.e. passive neutron, gamma emission and Cherenkov glow, are mainly due to minor actinides (e.g. Cm isotopes) and fission products (e.g. Cs isotopes). Their associated observables (i.e. measured counts or light) do not provide a direct measure of the residual fissile mass and are a complex function of several variables, such as irradiation history parameters. At the moment, none of the available methods allow a unambiguous determination of all the variables. Therefore, one typically supposes that one or more of such variables are actually known, so that the number of unknowns is reduced. An example of such case is the determination of the residual fissile content which can be estimated after the burnup of the fuel has been determined from the observables for example with a calibration procedure [7].

New NDA methods are being studied and developed in the last decade[3,8]. In an ideal scenario each method could generate one or more observables where each would allow the unique determination of the quantities of interest. However, this does not seem to be the case [9].

This situation therefore calls for a methodology to disentangle the quantities of interest from the observables.

In this framework, we carried out R&D work first to simulate observables associated to NDA equipment such as the ForkBall detector and SINRD. This work is described in Section 2, where the methodology developed at SCK•CEN to simulate observables is explained. Then, in Section 3 we focus on the interpretation of the data and the extraction of the quantities of interest from the simulated observables; we describe an approach based in neural network analysis. The obtained results are presented and discussed; outlook and recommendation for future work are given.

2. Detector response function simulations

2.1 Methodology

Due to the limited accessibility of spent fuel [10], the development and optimization of measurements methods are carried out by means of numerical calculations, often based on Monte Carlo methods [11]. Studies with Monte Carlo methods are based on models including the geometry and composition of the measurements equipment, the measurement environment and the characteristics of the radiation source.

The determination of the spent fuel composition and the characteristics of the emitted radiation can be achieved by means of evolution and depletion codes such as Origen-ARP [12,13,14] and ALEPH2 [15]. In the last years, SCK•CEN developed a spent fuel library (SFL) and investigated the impact of different factors on spent fuel composition and emitted radiation. The characteristics of spent fuel depend on quantities such as fuel type, irradiation

history and initial composition of the fuel. We focussed on 17x17 PWR fuel elements and studied the change of the neutron emission by varying parameters such as initial uranium enrichment (IE), average power level (AP), duration of the irradiation cycle (DIC) and cooling time between two complete irradiation cycles (CTIC), burnup (BU and cooling time (CT) after discharge [16,17]. The current version of the SFL contains information for Low Enriched Uranium (LEU) fuel with an initial enrichment between 2% and 5% and cases with Mixed Oxide (MOX) fuel with up to 10% of Pu. The data library does not contain information about fuel with burnable poison yet.

The spent fuel library consists of entries, each corresponding to a specific irradiation case. In one entry the total neutron emission, total gamma emission, and the corresponding energy spectra are given. In addition, the abundances of 50 selected nuclides are present [10]. The data are generated in a format which is compatible with the one of an MCNP [18] input file.

The overview of the methodology developed for this study is presented in Figure 1. The used methodology relies on the development of an MCNP input file template of the measurement setup, including the fuel. The composition of the fuel and the description of the source term is then taken from the library for the desired cases, substituted in the template and the simulation is run. More information on the specific tallies is given in the next section where the considered detection system and associated observables are described. The output file of the simulation is combined with the radionuclide abundancies and source term intensity obtained from the SFL to generate the database with signatures of the different fuel assemblies.

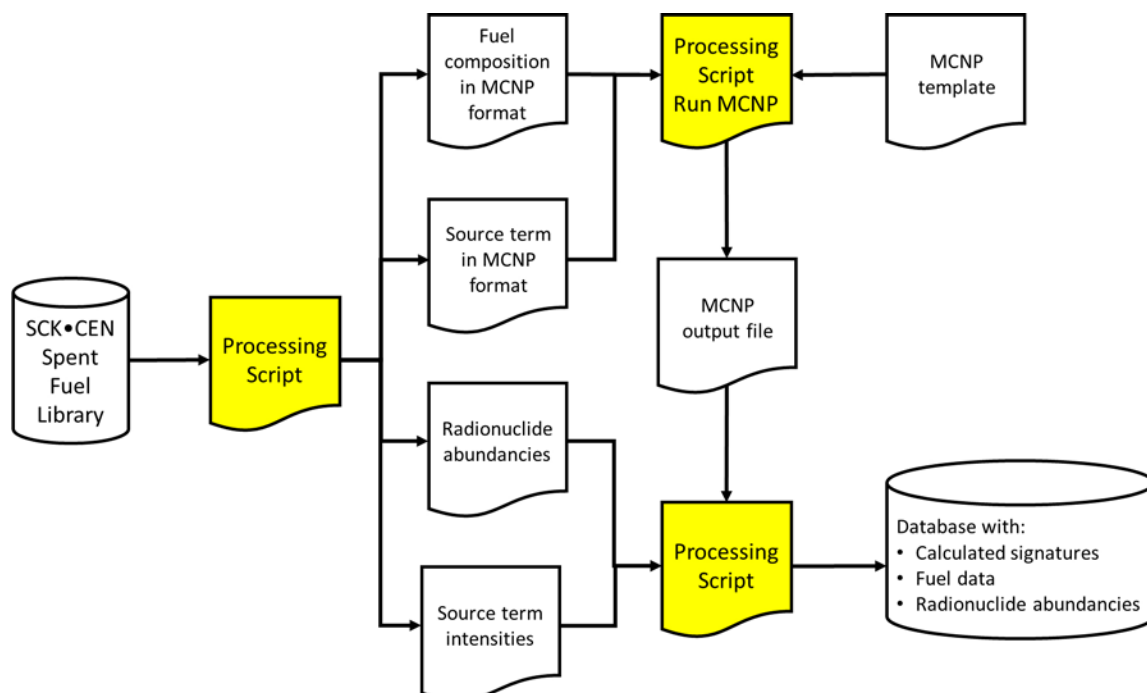


Figure 1: Overview of the methodology to generate simulated observables.

2.2 Considered detection systems

Two different types of equipment were considered. The first one is the so-called ForkBall detector [19]. This detector is designed for underwater measurements of SFA and includes features found in the Fork detector such as total neutron counts with fission chambers, total current obtained with ionization chambers and gamma-ray spectra obtained with a Cadmium Zinc Telluride (CZT) detector. The fission and ionization chamber are installed into cavities inside a polyethylene cylindrical arms wrapped with Cd. A variant without Cd was also considered.

The second detection systems implements the Self-Interrogation neutron resonance densitometry (SINRD) technique by carrying out measurements in dry conditions; this system features miniaturized fission chambers in the instrumentation channel of the SFA. The fission chambers are either bare or wrapped by neutron absorbing foils of Cd or Gd; additional details on the technique can be found in [8].

2.2.1 ForkBall detector

Separate simulations were carried out for neutrons and photons. In the neutron simulations for each entry of the SFL we determined the detection efficiency and the net multiplication factor both for the configuration with and without Cd around the polyethylene arms of the detector. The detection efficiency was estimated by multiplying to F4 tally by the (n,f) cross section of ²³⁵U and amount of fissile material in the fission chambers (FM treatment). The F4 tally is used to determine the neutron fluence per starting particle and the FM treatment allows to multiply this fluence by quantities such as cross sections and attenuation coefficients that depend on the cross section. With this treatment it is possible to determine the number of fissions associated to a given flux and a given amount of ²³⁵U and it is therefore possible to estimate the detector response.

While the neutrons simulations are straightforward and do not require a variance reduction technique, the gamma simulations associated to the CZT detectors require an ad-hoc procedure. Due to the presence of a shield and collimator used in the ForkBall, standard MCNP simulations are highly inefficient. A special procedure, described in [20], was therefore developed. The procedure splits the photon transport into two simulations. In a first simulation for a photon of given energy, the probability to reach CZT crystal is determined. A second set of simulations is done to determine the intrinsic detector efficiency that is the probability that an incoming photon deposits all its energy in the CZT crystal. These two quantities are then multiplied to obtain the overall full-energy detection efficiency, that is the probability that a photon of a given energy emitted by the fuel results in a full-energy peak in the crystal.

In first approximation, the overall full-energy detection efficiency does not depend on the fuel composition which still

largely made up of Uranium and Oxygen. The obtained results are given in Fig. 2.

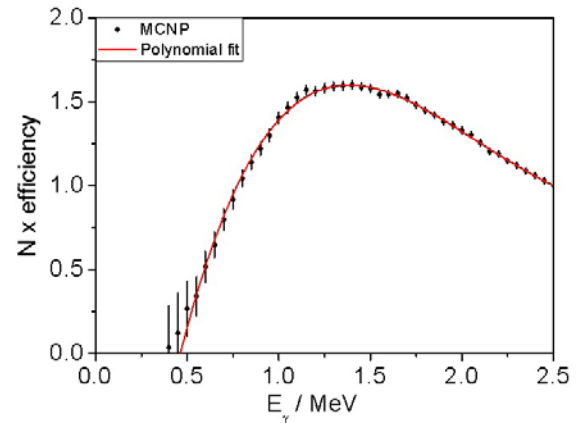


Figure 2: Normalised full-energy detection efficiency for the CZT detector in the Forkball detector.

The net peak count rate c due to a gamma ray of energy E_γ emitted by the radionuclide i is then given by

$$c(i, E_\gamma) = \varepsilon(E_\gamma) \times M_i \times A_i \times P(i, E_\gamma) \quad (1)$$

Where

- $\varepsilon(E_\gamma)$ is the overall full-energy detection efficiency
- M_i is the mass of the radionuclide in the SFA
- A_i is its specific activity
- $P(i, E_\gamma)$ is the number of emitted gamma rays of energy E_γ per decay

2.2.2 Self-Interrogation neutron resonance densitometry

For the SINRD technique the response of different types of fission chambers in the instrumentation channel of the SFA was simulated by multiplying the F4 tally by the (n,f) cross section of the active material and amount of fissile material in the fission chambers (FM treatment). The presence of shielding material was also accounted for by the FM treatment. Table 1 gives the details of the modelled detectors; more details on the choice of detectors and filters thickness are given in [8].

Active material	Filter	Energy cutoff
²³⁸ U	---	---
²³⁵ U	---	---
²³⁵ U	1 mm Cd	~ 1 eV
²³⁹ Pu	0.1 mm Gd	~ 0.1 eV
²³⁹ Pu	1 mm Cd	~ 1 eV

Table 1: Active materials and filters for SINRD.

As indicated in [8], the chosen signatures are sensitive both to ²³⁹Pu and ²³⁵U in the fuel.

The so-called SINRD signature and FAST to Thermal ratio (FAST/TH) are given in table 2. These quantities are

adimensional and are determined according to the procedure outlined in [8].

2.3 Data processing and results

The MCNP calculations provide observables (tallies) that are usually expressed per simulated source particles. To express the observables in absolute terms one has to take into account the source strength associated to the

considered spent fuel element. This information is retrieved from the SFL and the value of the observable is determined for the considered case. Overall a database of observables and spent fuel characteristics is generated. Within the database other calculated information on the spent fuel is also included such as the content of fissile material and the multiplication factor. An excerpt of the database content is shown in Table 2.

			Neutron	Counts			CZT			
BU	IE	CT	with Cd	without Cd	SINRD	FAST/TH	$^{134}\text{Cs}_1$	^{137}Cs	$^{134}\text{Cs}_2$	^{154}Eu
GWd/t _{HM}	%	y	cps	cps			cps	cps	cps	cps
5	2	5	1.0	1.2	0.026	0.009	22.2	425.2	38.4	3.2
10	2	5	6.3	6.9	0.031	0.010	88.3	847.3	153.2	12.9
15	2	5	31.3	34.4	0.037	0.009	187.3	1263.6	324.9	28.9
20	2	5	109.8	123.6	0.038	0.009	324.4	1677.7	562.7	51.2
25	2	5	284.2	317.0	0.041	0.009	485.4	2088.6	841.8	76.2
30	2	5	600.9	652.3	0.044	0.010	647.8	2490.3	1123.5	102.4
35	2	5	1088.2	1159.4	0.046	0.010	841.1	2893.2	1458.7	130.5
40	2	5	1711.4	1877.6	0.046	0.010	1041.0	3292.0	1805.4	157.4
45	2	5	2568.7	2793.7	0.047	0.010	1213.6	3679.9	2104.7	182.9
50	2	5	3559.5	3912.6	0.049	0.010	1420.1	4071.4	2462.8	208.8
55	2	5	4813.7	5240.8	0.049	0.010	1621.7	4459.6	2812.4	232.2

Table 2: Excerpt of the database. The signatures $^{134}\text{Cs}_1$ and $^{134}\text{Cs}_2$ denote the net peak areas at 605 keV and 796 keV respectively.

3. Neural network analysis

3.1 The use of Artificial Neural Networks as function approximators

Artificial neural networks (ANN) denote a class of computational models that emulate the functioning of the biological brain, by using a number of interconnected neural units (shortly, neurons or nodes). They have been widely used in machine learning and data mining, in particular owing to their capacity to work as universal function approximators, provided certain conditions are met by the network architecture [21].

An ANN can be described as a network in which each node i processes the n input units it is connected to through an transfer (or activation) function f_i :

$$y_i = f_i \left(\sum_{j=1}^n (w_{ij} \cdot x_j - \theta_i) \right) \quad (2)$$

where y_i is the output of neuron i , x_j is the j -th input to node i , w_{ij} is the weight of the connection between input j and node i , and θ_i is the threshold (or bias) of the node. While each neuron i can have its own transfer function in our implementation the same transfer function was used for all the neurons in a given layer.

Neural networks have a layer for input neurons, a layer for output neurons, and one or more inner layers of neurons,

also called hidden layers. Leshno et al. [21] proved that a standard multilayer feedforward (i.e. without feedback loops) ANN with a locally bounded piecewise continuous and non-polynomial transfer function can approximate any continuous function with any degree of accuracy. Feedforward networks used for function approximation problems have one or more hidden layers of nodes with non-linear transfer functions (e.g. sigmoid) followed by an output layer of nodes with linear transfer functions. This multilayer architecture allows the network to learn nonlinear relationships between input and output vectors.

Standard numerical optimisation algorithms can be used to optimise the network's performance function, often taken as the mean square error between the network's output and the network's target (real or simulated values of the function to be approximated). Various, gradient based or Jacobian based, learning algorithms [22] can be applied to adjust the weights and the biases of an ANN in a direction that optimises the performance function of the network. The most simple is the gradient descent algorithm, where the current vector $z^{(k)}$ of weights and biases is updated at each iteration $k+1$ based on the current gradient g_k and the learning rate α_k , until the network converges:

$$z^{(k+1)} = z^{(k)} - \alpha_k \cdot g_k \quad (3)$$

One of the fastest training algorithms for neural networks is the Levenberg-Marquardt optimization method [23], which was used for our application.

3.2 Spent fuel characterisation based on Artificial Neural Networks

In this work, we employ ANN's to explore the use of detector response values to characterize spent fuel in terms of

initial uranium enrichment, burnup and cooling time. Simulated data are used with different ANN architectures and learning algorithms. The MATLAB R2016b Neural Network Toolbox [24] was used for all data processing and analysis.

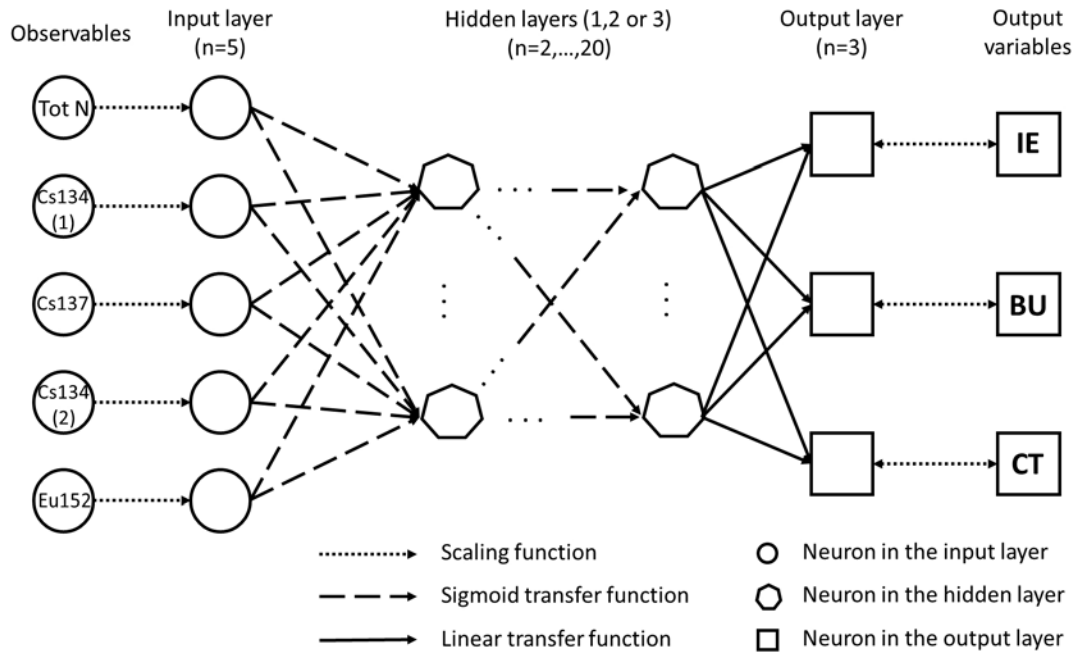


Figure 3: Artificial neural networks architecture implemented in this work.

The implemented ANN architecture is illustrated in Fig. 3. As observables, we considered total neutron counts for a Cd wrapped fission chamber and gamma rays spectroscopy data from ^{137}Cs , ^{134}Cs and ^{154}Eu . These data represent the variables in the input layer of the ANN. The BU, IE and CT represent the variables in the output layer of the ANN. While the BU and IE data were linearly spaced over their range, the CT data spanned several decades and had a logarithmical spacing. The natural logarithm was then taken to ensure that the resulting variable is uniformly distributed over its range. Both the values in the input layer (observable) and the one in the output layer (quantity to be predicted) were scaled between -1 and $+1$ before being fed to the network optimization algorithm.

The algorithm was applied on a subset of the database described in section 2.3. We considered data with fourteen burnup (BU) values (from 5 to 70 GWd/t_j in steps of 5 GWd/t_j), initial enrichment (IE) of between 2.0% and 5.0% in steps of 0.5%, eleven values of cooling time (CT) from 1 day to 100 years. A total of 1078 cases were considered.

For the neurons in the hidden layers we used hyperbolic tangent sigmoid transfer functions whereas for the transfer functions for the output neurons were linear. The quantity

mean square error (*mse*) was used as target for minimisation. In the used *mse* each squared error contributes with the same importance as follows:

$$mse = \frac{1}{3N} \sum_{j=1}^3 \sum_{k=1}^N (A_{k,j,calc} - A_{k,j})^2 \quad (4)$$

Where $A_{k,j,calc}$ is the value of the parameter as determined by the ANN in the output layer (Fig. 3), $A_{k,j}$ is the nominal value of the parameter. The index j runs over the IE, BU and CT output while k runs over the part of the database used for training. The calculation of the *mse* is done before the final scaling.

In the future we will define the performance in such a way that the percentage deviation enters in the definition of the quantity to be minimized rather than the absolute deviation. Note that the absolute variation in the logarithm of CT results already in a relative deviation on the CT.

The database of simulated observables and spent fuel characteristics is divided in two sets, corresponding to training and validation. The data in the validation set are used to stop training if the network performance on these data fails to improve or remains the same for a predefined number of iterations. The Levenberg-Marquardt algorithm

was used for training the network. The neural networks tested used up to three hidden layers.

3.3 Results

First we studied the impact of the number of neurons on the performance, assuming that all data set was used to train the network. The performance was then calculated

on the whole database of N=1078 cases. We considered from 2 to 20 neurons per hidden layer, while the number of hidden layers went from one to three. The obtained results indicate that the performance increases in general with the number of neurons per layer and with the number of hidden layers. However, the improvement is marginal above 15 neurons, as shown in Fig. 4.

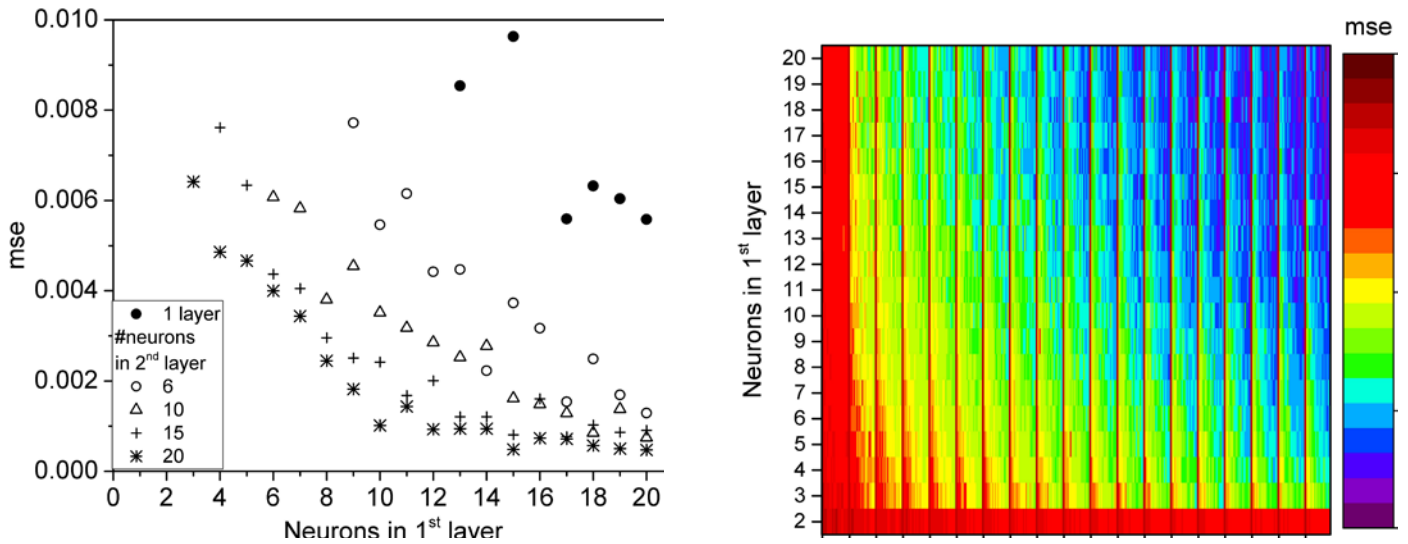


Figure 4: mse for ANN with one, two and three hidden layers as a function of the number of neurons. The mse in the right figure is limited to a maximum value of 0.01.

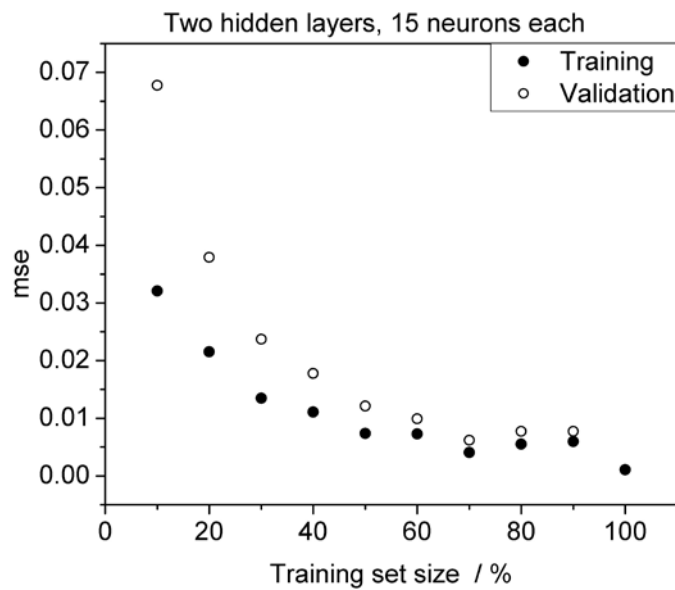


Figure 5: mse for ANN with two hidden layers as a function of the training set size. For both hidden layers the number of neurons was set to 15.

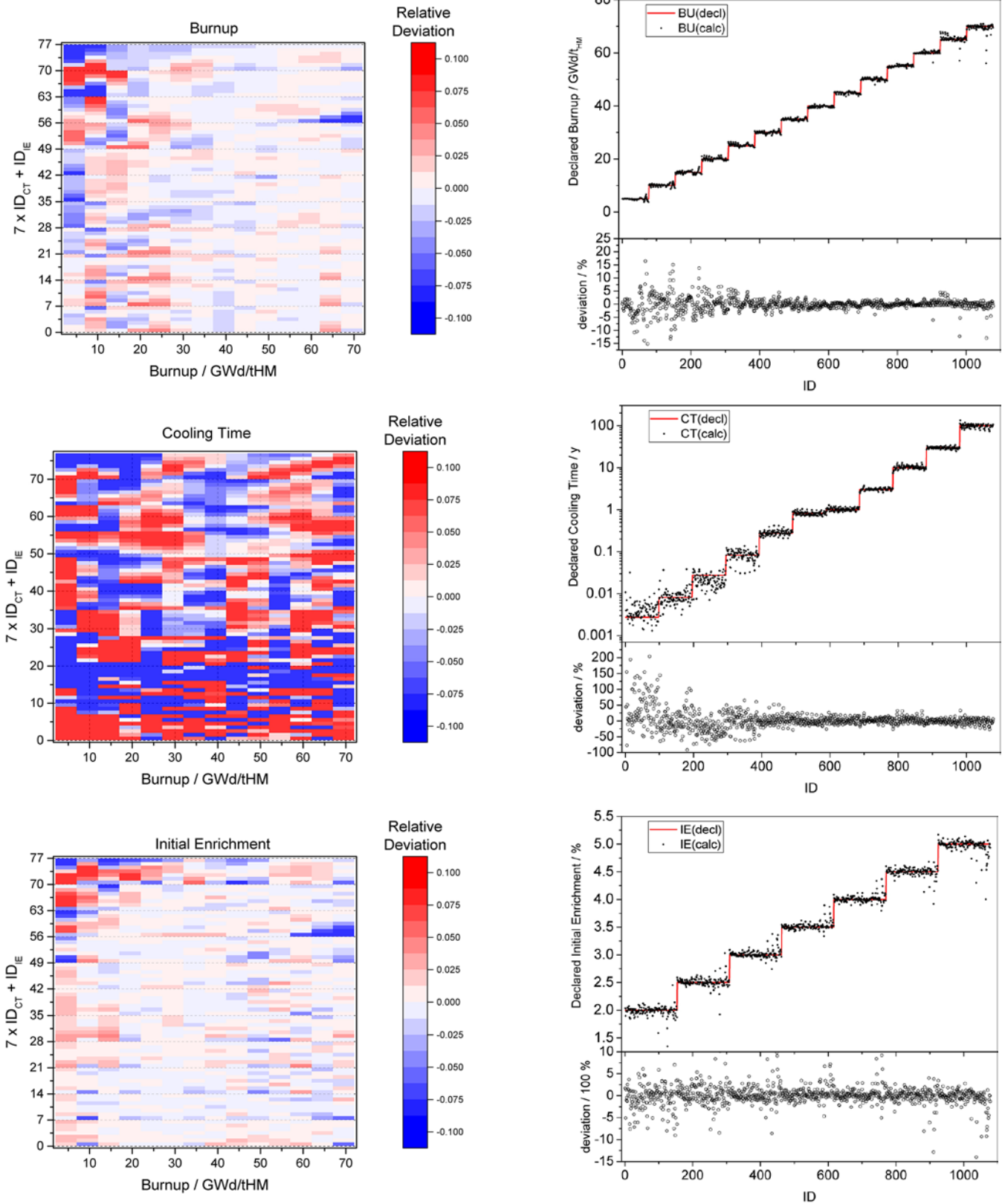


Figure 6: Deviations in the predicted values of BU, IE and CT for the considered cases. The results refer to an ANN with 3 hidden layers and 20 neurons per layer. The training set size was 50%. See the text for explanation.

In addition, we carried out calculations by changing the fraction of data used for training from 10% to 100% in step of 10%. The number of neurons was 5, 10, 15 and 20 and we considered up to three hidden layers; both the performance on the training and the validation set were computed. The assignment of individual data to the training or validation set was done randomly by MATLAB.

In general, we found that the value of the performance changes if the calculation is repeated; this is due to the fact that in the current implementation the initial values of the weights and biases of the ANN are randomly assigned [25] and this is affecting the results. For each network configuration the calculations were repeated 20 times and the average performance was calculated with its standard deviation. For the case in which 100% of the data are used for training, we observed a standard deviation in the *mse* between 12 % and 25%. By reducing the share of the training set, the standard deviations are higher; this is due to the fact that choice of the data used for training is random and changes every time; consequently, the value of the performance is affected. In addition, it was found that also the share of the training and validation data sets is not a fixed number but fluctuates around its nominal values. The resulting spread on the performance should be kept in mind when comparing different performance values.

The performance on the training set was in general better than the performance on the validation set. The difference between them was increasing by reducing the size of the training set, as shown in Fig. 5., and by increasing the number of neurons in the last hidden layer.

As expected the performance improves with the size of the training set and there is a clear difference between the performance obtained with 90% and 100% training; however, the improvement is marginal in the range 50% to 90%.

While it is of interest to identify which parameters affect the performance, it is also important to understand how performance values translate into deviation between calculated values and “real” values of BU, IE and CT. In Fig. 6, the % deviation on the value of BU, CT and IE are shown for the ANN with 3 hidden layers and 20 neurons per hidden layer with 50% training. In the plots on the left, the deviations are shown as a function of BU (X-axis) and IE and CT (Y-axis). The Y-axis is an identification number ID that is given by the formula $7 \times ID_{CT} + ID_{IE}$, where ID_{CT} and ID_{IE} range from 1 to 11 and 1 to 7 respectively and uniquely identify the case of CT and IE to which they refer. For the plots on the right the deviations are given as a function of an arbitrary case identified number (ID) that is used for a more straightforward representation; for each variable (BU, CT, IE) the ID is chosen such that the corresponding declared variable is monotonically increasing.

The results indicate that if 20 neurons and 50% of the data are used for training the ANN is capable of reproducing the value of BU within 3% for 85% of the cases, the value of IE within 2% for 80% of the cases and the value of CT within 10% for 58% of the cases.

In a more ideal case, where 100% of the data are used for training, the ANN is capable of reproducing the value of BU within 3% for 96% of the cases, the value of IE within 2% for 98% of the cases and the value of CT within 10% for 87% of the cases.

The reason why we obtain larger deviation on the CT when compared to BU and IE is not clear. The larger deviations at low value of CT can be related to the choice of observables which are less sensitive to CT smaller than 1 y.

4. Conclusions and outlook

In this work we first reported about a methodology developed to simulate detector response functions for different types of NDA instruments. A database of detector responses for 8400 cases with different fuel characteristics and irradiation parameters was then obtained. The use of the simulated observables as input for data analysis algorithms aims at uniquely characterizing the spent fuel and drawing safeguards conclusions. We explored the application of artificial neural networks due to their ability to generalize non-linear relationships on a subset of data corresponding to cooling times smaller than 100 years.

We studied the network performances in terms of mean square error as a function of the number of hidden layers, number of neurons in each hidden layer and share of the training data set. We could conclude that, within the range considered, the performances increase with the number of neurons, number of hidden layers and share of the training data set. The results show that, when all the data set is used for training, the ANN is able to reproduce the BU and IE within a few percent for most of the analysed cases, whereas the resulting CT has a larger deviation especially for values lower than 1y. The performance is significantly worse when a fraction lower than 50 % of the data set is used for training the ANN.

Future research will focus on improving the performance of the network with respect to the CT and further testing of the optimal network configuration. In particular, the performance of the network when selecting CT larger than 1 y or 10 y will be investigated. The possibility to selectively use data for training rather than randomly choose the data will also be considered. We will investigate the impact of the initial weight values. We will also try to identify which additional observables (for instance the SINRD signature) would result in an improvement of the performance. The impact of the range values of burn-up, initial enrichment and cooling time on the

performance will also be studied. The use of different performance functions will also be considered.

5. Legal matters

5.1 Privacy regulations and protection of personal data

"I agree that ESARDA may print my name/contact data/ photograph/article in the ESARDA Bulletin/Symposium proceedings or any other ESARDA publications and when necessary for any other purposes connected with ESARDA activities."

5.2 Copyright

The authors agree that submission of an article automatically authorises ESARDA to publish the work/article in whole or in part in all ESARDA publications – the bulletin, meeting proceedings, and on the website.

The authors declare that their work/article is original and not a violation or infringement of any existing copyright.

6. References

- [1] D. Reilly, N. Ensslin, H. Smith Jr. and S. Kreiner, *Passive Nondestructive Assay of Nuclear Materials*, NUREG/CR-5550, LA-UR-90-732, 1991
- [2] *Coordinated Technical Research Meeting on Spent Fuel Verification Methods*, IAEA March 3-6 2003
- [3] S. Tobin, H. Menlove, M. Swinhoe, M. Shear, *Next Generation Safeguards Initiative research to determine the Pu mass in spent fuel assemblies: Purpose, approach, constraints, implementation, and calibration*, Nuclear Instruments & Methods In Physics Research Section A, 2011, doi 10.1016/j.nima.2010.09.064
- [4] Park W. S., et al., 2014. "Safeguards by design at the encapsulation plant in Finland". Proceedings of the 2014 IAEA safeguards symposium.
- [5] European Council Decision 2006/976/Euratom of 19 December 2006
- [6] IGD-TP Implementing Geological Disposal of Radioactive Waste Technology Platform Strategic Research Agenda, www.igdtp.eu/index.php/documents/doc_download/14-strategic-research-agenda, 2011, ISBN 978-91-979786-0-6,
- [7] Borella A., et al., *Spent Fuel Measurements with the Fork Detector at the Nuclear Power Plant of Doel*, 33rd ESARDA Annual Meeting, Budapest, Hungary, May 16-20 2011
- [8] R. Rossa, *Advanced non-destructive methods for criticality safety and safeguards of used nuclear fuel*, PhD thesis at Université libre de Bruxelles, September 2016.
- [9] S. Tobin et al., *Research into Measured and Simulated Nondestructive Assay Data to Address the Spent Fuel Assay Needs of Nuclear Repositories*, In: Proc. 57rd INMM Annual Meeting, Atlanta, Georgia, United States, 2016
- [10] A. Borella, et al., *Extension of the SCK•CEN spent fuel inventory library*, 37th ESARDA Annual Meeting, 2015
- [11] M.H. Kalos and P.A. Whitlock, *Monte Carlo Methods. Volume I: Basics*, John Wiley & Sons, NY 1986.
- [12] S.M. Bowman , O.W. Hermann, L.C. Leal, C.W. Parks, *ORIGEN-ARP, A Fast and Easy-to-Use Source Term Generation Tool*, ORNL/CP-104231, Oak Ridge 1999
- [13] I. Germina, et al. *Overview of ORIGEN-ARP and its Application to VVER and RBMK*. Oak Ridge National Laboratory, Oak Ridge, TN, 2007
- [14] I. Gauld, S. Bowman, J. Horwedel, *Origen-ARP: automatic rapid processing for spent fuel depletion, decay, and source term analysis*, ORNL/TM-2005/39. January 2009
- [15] A. Stankovskiy, G. van den Eynde *ALEPH 2.2 A Monte Carlo Burn-up Code*, SCK•CEN-R-5267, September 2012
- [16] R. Rossa., et al., *Development of a reference spent fuel library of 17x17 PWR fuel assemblies*, ESARDA BULLETIN, No. 50, December 2013
- [17] A. Borella, M. Gad, R. Rossa, K. van der Meer, *Sensitivity Studies on the Neutron Emission of Spent Nuclear Fuel by Means of the Origen-ARP Code*, In: Proceeding of the 55th INMM Annual Meeting, Atlanta, Georgia, United States, July 2014.
- [18] MCNP6 Users Manual - Code Version 6.1.1 beta, LA-CP-14-00745, June 2014.
- [19] A. Borella, et al., *Advances in the Development of a Spent Fuel Measurement Device in Belgian Nuclear Power Plants.- In: Symposium on International Safeguards, Linking Strategy, Implementation and People*, Book of Abstracts, Presentations and Papers, 2014, IAEA, Vienna, Austria, p. 272
- [20] A. Borella, et al., *A Method To Determine Detector Response Functions In A Heavily Shielded Environment And Application To Spent Fuel Measurements With Cadmium Zinc Telluride Detectors*, In: MC2015 - Joint International Conference on Mathematics and Computation (M&C), Supercomputing in Nuclear Applications (SNA) and the Monte Carlo (MC) Method, Nashville, United States, 2015

- [21] Leshno, M., Lin, V. Y., Pinkus, A., & Schocken, S., *Multilayer feedforward networks with a nonpolynomial activation function can approximate any function*, *Neural networks*, 6(6):861-867, 1993.
- [22] Hagan M.T., Demuth H.B., Beale M.H., *Neural Network Design*, Boston, MA: PWS Publishing, 1996.
- [23] Hagan, M.T., and M. Menhaj, *Training feed-forward networks with the Marquardt algorithm*, *IEEE Transactions on Neural Networks*, Vol. 5, No. 6, 1999, pp. 989–993, 1994.
- [24] <https://www.mathworks.com/products/neural-network.html>
- [25] MATLAB documentation, *init* function